Radio Science, Volume 16, Number 5, pages 917–925, September–October 1981

Sea state frequency features observed by ground wave HF Doppler radar

P. Forget, P. Broche, and J. C. De Maistre

Laboratoire de Sondages Electromagnétiques de l'Environnement Terrestre, Université de Toulon 83130 La Garde, France

A. Fontanel

Institut Français du Pétrole, 92506 Rueil-Malmaison, France

(Received May 21, 1980; revised March 11, 1981; accepted March 13, 1981.)

This paper investigates the relationship between the frequency features of the directional spectrum of ocean waves (cutoff frequency and peak frequency of wind waves, frequency of quasi-monochromatic swell) and the properties of the spectrum of the sea echo obtained by HF Doppler radar. A theoretical analysis is performed to check the validity of a simple result that states that at upper HF, a long-wave spectral feature at frequency F_0 affects the radar echo at frequencies $\pm f_B \pm F_0$ on either side of the Bragg lines at $\pm f_B$ corresponding to resonant backscattering of radio waves with a given wavelength by half-wavelength ocean waves. An experiment using both radar and standard in situ measurements for several weeks at different times of the year shows that this relationship can be used to formulate a method for estimating the frequency features of the sea with suitable accuracy.

1. INTRODUCTION

More than 20 years ago, the special spectral properties of high-frequency electromagnetic waves backscattered by the surface of the sea suggested that it might be possible to use HF radar to investigate wave fields on the surface of the ocean [*Crombie,* 1955]. There is indeed a correlation, because of the interaction of electromagnetic waves and ocean surface waves, between the Doppler spectrum of the radar echo and the directional spectrum of the sea. This directional spectrum can be fully extracted by the complete inversion of the radar echo, although with some difficulty [*Lipa,* 1978]. Nevertheless, many users who cannot operate standard in situ sensors (buoys, etc.) because of technical or economic constraints need some overall parameters of the sea state, and therefore it is of interest to study specific ways of estimating these parameters: wind direction [*Long and Trizna,* 1973; *Stewart and Barnum,* 1975; *Broche,* 1979], significant wave height and dominant period [*Barrick,* 1977*a*], swell characteristics [*Tyler et al.,* 1972; *Lipa and Barrick,* 1980], and surface currents [*Stewart and Joy,* 1974; *Barrick et al.,* 1977].

This paper deals with estimating the main frequency-characteristic features of the sea spectrum, i.e., the cutoff and dominant frequency of wind waves and the frequency of swell.

The general appearance of the Doppler spectra observed (Figure 3) is correctly described by current models of the interaction between the sea surface and HF electromagnetic waves, and especially by the models developed by *Barrick* [1972]. This appearance can be expressed by

$$E(f_d) = E^{(1)}(f_d) + E^{(2)}(f_d)$$

in which f_d is the Doppler shift between the frequency of the radio wave received and that of the wave transmitted.

$E^{(1)}(f_d)$ represents the so-called 'first-order' echo which occurs in the form of two quasi-monochromatic lines ('Bragg lines') whose positions, which are symmetrical in relation to zero frequency, are given by

$$f_d = \pm f_B = \pm(2gk_t)^{1/2}/2\pi$$

where g is the acceleration of gravity and k_t the wave number of the incident electromagnetic waves.

$E^{(2)}(f_d)$ represents the so-called 'second-order' echo which is a continuum observed between and on either side of the Bragg lines. *Barrick* [1977*b*] showed that for sufficient sea heights it may be expressed as

Paper number 1S0450.
0048-6604/81/0910-0450$01.00

$$E^{(2)}(f_d) = A\,w(f_d)\,S(|f_B - f_d|)/\int E^{(1)}(f_d)\,df_d$$

A is a known constant coefficient; $S(F)$ is the nondirectional wave height frequency spectrum of ocean waves; and w is a weighting function that depends only to a very slight extent on sea state but is somewhat dependent on the angle θ between the direction of the radar beam and the dominant propagation direction [*Barrick,* 1977*b*].

The second-order spectrum would then reproduce, on either side of the Bragg lines and in proportion to the energy of these latter, the $S(F)$ spectrum weighted by function w. This result should be compared with the one given by *Hasselmann* [1971] to the extent that function $w(f_d)$ is found to be almost constant in a frequency range around f_B (almost $0.5f_B < f_d < 1.4f_B$).

Specific spectral properties of the sea state observed at a given frequency F_0 could then be related to the behavior of the spectrum of the second-order echo at the following frequencies:

$$f_0 = \pm f_B \pm F_0$$

This equation is investigated in detail from its theoretical standpoint, and its use for estimating specific F_0 frequencies is compared with the results of in situ measurements made with standard sensors (buoys). The investigation has to do with the cutoff frequency and the dominant frequency of wind waves and with the frequency of quasi-monochromatic swell.

2. THEORETICAL CONSIDERATIONS

It has been stated that the equation for the Doppler spectrum of the radar echo may be written as [*Barrick,* 1972]

$$E^{(1)}(f_d) = \alpha_1 S(-2\varepsilon\vec{k}_i)\delta(f_d - \varepsilon f_B) \qquad \varepsilon = \pm 1$$

where α_1 is a numerical constant; δ is the Dirac function; and $S(\vec{K})$ is the directional spectrum of the waves with wave vector $\vec{K}$, and as

$$E^{(2)}(f_d) = \alpha_2 \sum_{\varepsilon_1,\varepsilon_2} \int\int T(\vec{K}_1, \vec{K}_2) S(\varepsilon_1 \vec{K}_1) \cdot S(\varepsilon_2 \vec{K}_2)\delta(f_d - \varepsilon_1 F_1 - \varepsilon_2 F_2)\,d\vec{K}_2$$

where α_2 is a numerical coefficient; $\vec{K}_1$ and $\vec{K}_2$ are the wave vectors of the waves having frequencies F_1 and F_2, which fulfill the following condition:

$$\vec{K}_1 + \vec{K}_2 = -2\vec{k}_i$$

T is a coupling coefficient, and ε_1, $\varepsilon_2 = \pm 1$, with the summation being done on the four combinations for ε_1 and ε_2. Detailed expressions for α_1, α_2, and T are given in the hereabove referred to paper [*Barrick,* 1972]. Since each component satisfies the standard dispersion equation $(2\pi F)^2 = gK$, the relation between $\vec{K}_1$ and $\vec{K}_2$ implies a relation between F_1 and F_2 which is illustrated in Figure 1. Depending on the direction of $\vec{K}_1$ in relation to that of $\vec{k}_i$, F_2 is in a range limited by two extrema corresponding to $\vec{K}_1$ parallel to $\vec{k}_i$ (minimum) and

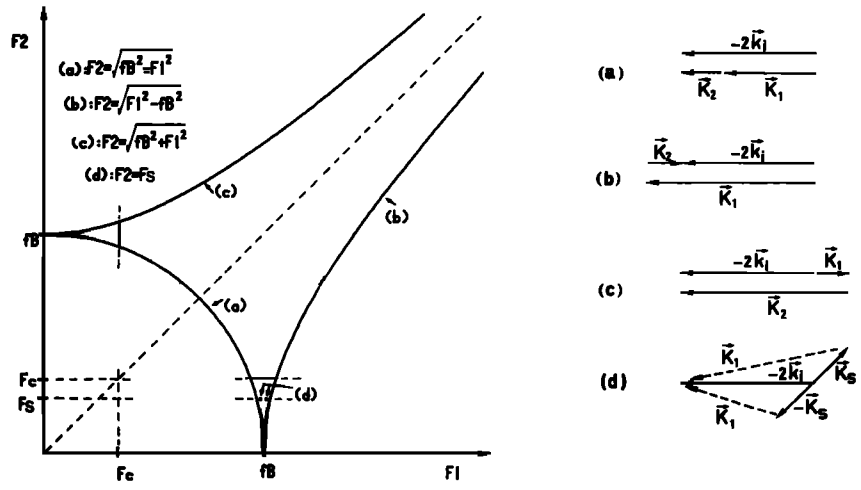

Fig. 1. Area of the (F_1F_2) plane contributing to the second-order echo (limited by curves *a*, *b*, and *c* and $F_1 > F_c$, $F_2 > F_c$). Curves *a*, *b*, and *c* are associated with the spatial configurations shown on the right. Curve *d* concerns the case of swell for which only two interactions are possible.

to $\vec{K}_1$ antiparallel to $\vec{k}_i$ (maximum). Then:

$$|f_B^2 - F_1^2|^{1/2} < F_2 < (f_B^2 + F_1^2)^{1/2}$$

Furthermore, if F_c is the cutoff frequency in the wave spectrum below which wave energy is negligible, a contribution to the integral in $E^{(2)}(f_d)$ can originate only in the region where F_1 and F_2 are greater than F_c.

A wave having the frequency F_1 makes a contribution to the Doppler spectrum at the frequencies $f_d = \varepsilon_1 F_1 + \varepsilon_2 F_2$ which, for each choice of ε_1 and ε_2, belong to a range that is deduced from the previous one by a simple transformation. This range is shown in Figure 2 for $f_d > 0$ and for the following choices:

$f_d > f_B$ (sum interactions)

$$\varepsilon_1 = +1 \qquad \varepsilon_2 = +1$$

and

$f_d < f_B$ (difference interactions)

$$\varepsilon_1 = +1 \qquad \varepsilon_2 = -1$$

or

$$\varepsilon_1 = -1 \qquad \varepsilon_2 = +1$$

The inequalities above obviously imply that some energy is present in all the directions and therefore that the directional pattern of the wave energy is smooth enough.

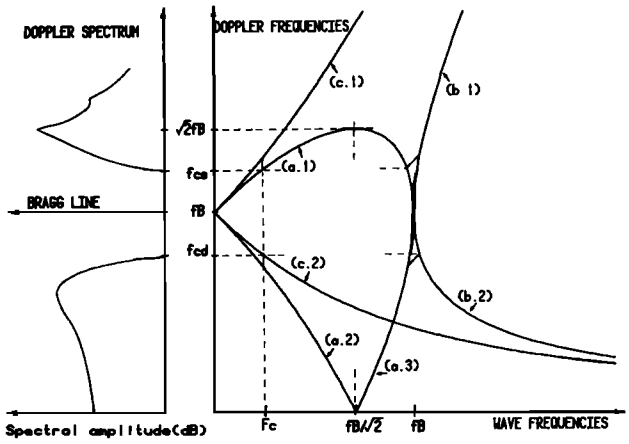

Fig. 2. Zones of correspondence between wave frequencies F_1 and Doppler frequencies f_d. The limit curves $(a.1)$, $(b.1)$, and $(c.1)$ are deduced from those in Figure 1 by the following transformations: $(a.1) \equiv f_d = F_1 + (a)$; $(a.2) \equiv f_d = -F_1 + (a)$; $(a.3) \equiv f_d = F_1 - (a)$; $(b.1) \equiv f_d = F_1 + (b)$; $(b.2) \equiv f_d = F_1 - (b)$; $(c.1) \equiv f_d = +F_1 + (c)$; $(c.2) \equiv f_d = -F_1 + (c)$. The cutoff in the wave spectrum is correlated to the cutoff in the Doppler spectrum at frequencies f_{cs} and f_{cd}.

Figure 2 can be used either to evaluate the spectral range to which a wave having the frequency F_1 contributes or to determine the set of waves contributing to a given Doppler frequency f_d.

Under these conditions, a cutoff appears at the following frequencies:

$$\begin{aligned} f_{cs} &= F_c + (f_B^2 - F_c^2)^{1/2} \quad \text{for } f_d > f_B \quad (\text{curve } a.1) \\ f_{cd} &= -F_c + (f_B^2 + F_c^2)^{1/2} \quad \text{for } f_d < f_B \quad (\text{curve } c.2) \end{aligned} \tag{1}$$

If the experimental parameters and the sea state are such that $F_c/f_B < 1$ (or $K_c/2k_i \ll 1$, with K_c being the wave number corresponding to frequency F_c), a second-order development in F_c/f_B gives

$$\begin{aligned} f_{cs} &= f_B + F_c(1 - F_c/2f_B) \\ f_{cd} &= f_B - F_c(1 - F_c/2f_B) \end{aligned}$$

whereas the simplified theory referred to in the introduction would lead to

$$\begin{aligned} f_{cs} &= f_B + F_c \\ f_{cd} &= f_B - F_c \end{aligned} \tag{2}$$

In practice, if L_c is the width of the second-order spectrum between the Bragg lines ($L_c = 2f_{cd}$), F_c can be estimated by inverting (1) or (2) in this way:

$$\begin{aligned} F_c'' &= (4f_B^2 - L_c^2)/4L_c \\ F_c' &= f_B - L_c/2 \end{aligned} \tag{3}$$

In principle, F_c'' gives the exact value for F_c, and F_c' is an underevaluation of F_c with a difference of about $F_c/2f_B$. The approximation given by F_c' is then better as long as F_c is low (great wave heights) and f_B is high (high radar frequency).

From the theoretical standpoint, a simple relation, such as the one that is valid for cutoff frequencies, does not exist between the dominant frequency in the wave spectrum, F_m, and the frequency of the maximum amplitude in the Doppler spectrum. All that can be said is that a scale distortion exists between the wave spectrum $S(F)$ and the Doppler spectrum $E^{(2)}(|f_d \pm f_B|)$, a distortion which can be analytically evaluated for the cutoff frequencies f_c and F_c alone. Nevertheless, the theoretical considerations given in the introduction together with considerations based on experimental findings suggest that the arguments presented above are still valid and that it should be possible to estimate the

dominant frequency in the wave spectrum by measuring the width L_m of the second-order echo between the Bragg lines as measured between the two relative maxima of this spectrum by

$$F'_m = f_B - L_m/2$$
$$F''_m = (4f_B^2 - L_m^2)/4L_m \quad (4)$$

3. EXPERIMENTAL CONDITIONS

Two different sites were used for the experimental campaigns from 1977 to 1979.

The first one, in the western Mediterranean Sea, has been described previously [*De Maistre et al.*, 1978] along with the mean features of the radar. Meteorological conditions varied considerably, and several weeks of measurements in June and December 1977 and in March 1978 revealed very different conditions for the wind-driven sea with regard either to amplitude or to the dominant direction of wave propagation. An anemometer placed on a buoy moored close to the area covered by the radar and a Waverider buoy tied to the first one have given data on the actual sea conditions (wave height, nondirectional spectrum, wind speed and direction).

The second one, in the Atlantic Ocean near the mouth of the Gironde River, was used in June 1979, with a similar radar. The amplitude of the wind-driven sea was generally low (wind speed less than 15 kn (27.8 km/h)), the wind direction was very stable, and swell was a quasi-permanent phenomenon. Actual sea conditions were monitored by a pitch-and-roll buoy operated by the French group Centre Océanologique de Bretagne–Centre National d'Exploitation des Océans (COB-CNEXO) and giving the dominant direction of propagation for each frequency in the wave spectrum.

At both stations, the radar devices operated at frequencies in the vicinity of 6 and 12 MHz, and the target was a patch of sea with a radial extent of 15 km and a width of a few kilometers. The patch was situated almost 40 km from the shore. Each spectrum is the result of incoherent summations of four or eight consecutive spectra, each recorded over a time of 164 s. Only the spectra having symmetrical cutoff frequencies between the Bragg lines were taken into consideration for estimating F_m and F_c, as was said in section 2. An example is given in Figure 3.

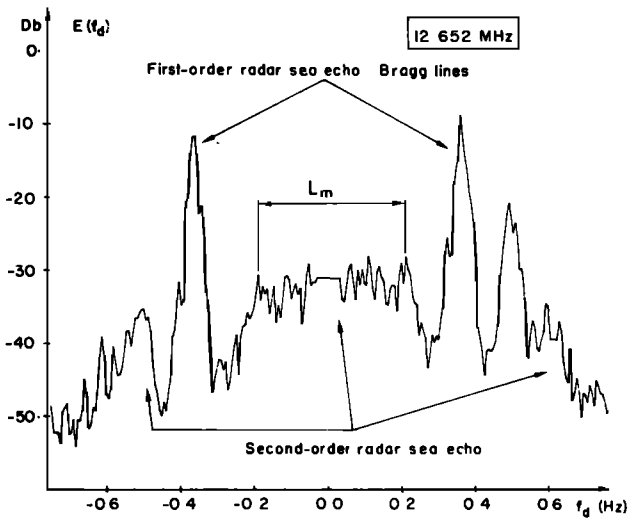

Fig. 3. An example of experimental Doppler spectrum at 12.652 MHz.

4. EXPERIMENTAL RESULTS AND DISCUSSION

Figure 4 gives the experimental results in the form of the estimate F'_m or F''_m as a function of the value of F_m measured in situ by the buoy. It can be seen on the average that

$$F'_m < F_m \quad \text{and} \quad F''_m > F_m$$

However, the difference in $|F_m - F'_m|$ is much smaller than $|F''_m - F_m|$, and so it appears that F'_m is a better estimate than F''_m, at the opposite of what was theoretically expected for the cutoff frequency F_c. For $F_m \leq 0.25$ Hz, the mean deviation of $F''_m - F_m$ is 0.062 Hz and that of $F'_m - F_m$ is -0.006 Hz only.

Figure 4 also confirms that the quality of the estimate increases as F_m decreases (i.e., in general as the wave height becomes higher). A few results at a radar frequency of 6 MHz, not shown in the figure, also show that the estimate is all the better as f_B is higher. *Barrick* [1977*a*, *b*] already pointed out that measurements obtained by using the weighting function were subjected to the same constraints.

An approximation of the significant wave height, H 1/3, can be deduced from F_m for a fully risen sea. Indeed there is a relationship between F_m and H 1/3, and for the Pierson-Moskowitz model it is

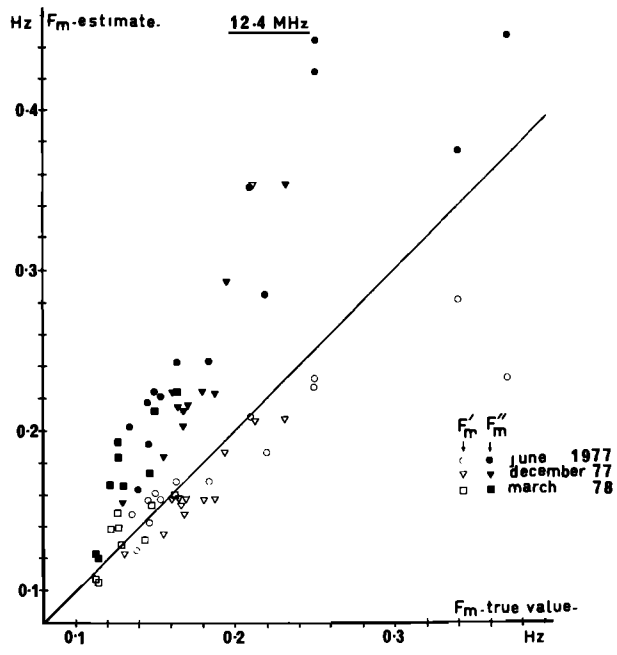

Fig. 4. F_m inversion for experimental data. Radar frequency is about 12.4 MHz. Various sea state conditions have been considered. The 'true value' is measured by the Waverider buoy.

$$H\,1/3 = 0.04/F_m^2$$

Actually, the diversity of the meteorological conditions occurring while the data were being collected (fully developed sea, increasing or decreasing sea state, limited fetch or limited interaction time situations, presence of swell) restricts the validity of such an equation. This greatly influences the quality of the estimate of H 1/3, as is shown by the spread of the experimental points in Figure 5, where the estimated value of H 1/3 is plotted as a function of the value measured by the buoy.

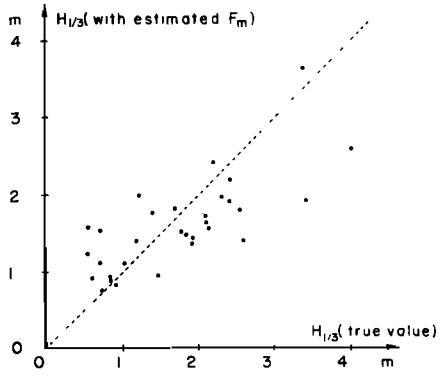

Fig. 5. H 1/3 inversion using $H\,1/3 = 0.04/F_m^2$, where F_m is estimated from second-order radar sea echo. These values are compared with the true values, as determined by a Waverider buoy.

5. SPECIAL CASE OF SWELL

When there is a swell (i.e., quasi-monochromatic and monodirectional low-frequency waves), the contribution of the swell may be separated from that of the wind-driven sea. The spectrum of the sea state may be written as

$$S(\vec{K}) = S_W(\vec{K}) + S_S(\vec{K})$$

The product $S(\varepsilon_1\vec{K}_1) \cdot S(\varepsilon_2\vec{K}_2)$, which belongs to the expression for $E^{(2)}(f_d)$, can be developed in the form

$$S_W \cdot S_W + S_W(\varepsilon_1\vec{K}_1)S_S(\varepsilon_2\vec{K}_2) + S_W(\varepsilon_2\vec{K}_2)S_S(\varepsilon_1\vec{K}_1) + S_S \cdot S_S$$

The first term contributes to a second-order echo that is identical to the one that would be observed in the absence of swell. The last term leads to a zero result because the condition $\vec{K}_1 + \vec{K}_2 = -2\vec{K}_i$ cannot be fulfilled by a monochromatic swell having sufficiently low frequency. The other two terms make equal contributions, and their sum is

$$E_S^{(2)}(f_d) = 2\alpha_2 \sum_{\varepsilon_1,\varepsilon_2=\pm 1} \int\int T \cdot S_W(\varepsilon_1\vec{K}_1)S_S(\varepsilon_2\vec{K}_2)\delta(f_d - \varepsilon_1 F_1 - \varepsilon_2 F_2)\,d\vec{K}_2$$

If the swell is perfectly monochromatic with a frequency of F_S, a wave vector of $\vec{K}_S$, and a mean square wave height of h, it can be written as

$$S_S(\vec{K}) = h^2\delta(\vec{K} - \vec{K}_S)$$

The area contributing to $E_S^{(2)}$ in the diagram in Figure 1 is restricted to two points, corresponding to $F_2 = F_S$, and to the two possibilities $\vec{K}_2 = \varepsilon_2\vec{K}_S$. The swell is then correlated with four monochromatic lines in the second-order echo. Moreover, the integral is immediately computed, and

$$E_S^{(2)}(f_d) = 2\alpha_2 h^2 \sum_{\varepsilon_1,\varepsilon_2=\pm 1} \cdot T(\vec{K}_1, \vec{K}_S)S_W(\varepsilon_1\vec{K}_1)\delta(f_d - \varepsilon_1 F_1 - \varepsilon_2 F_S)$$

with

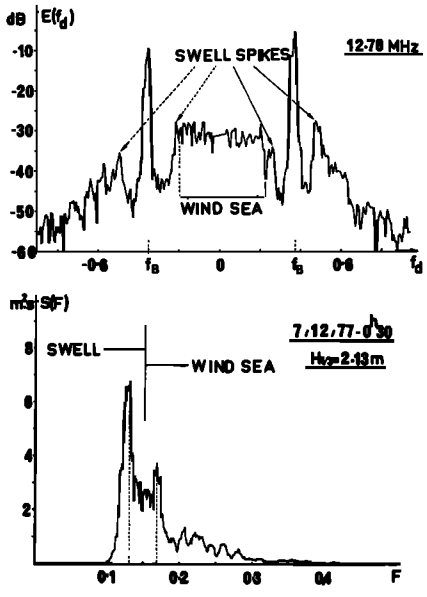

Fig. 6. Example of Doppler spectrum showing at least two swell spikes, with the corresponding wave spectrum (measured by a buoy in the Mediterranean Sea). The structure of the Doppler spectrum is coherent with an interpretation of the wave spectrum in terms of two wave systems, i.e., waves of the wind sea and swell.

$$\vec{K}_1 = -2\vec{k}_i - \epsilon_2 \vec{K}_S$$

If K_S and θ are the modulus and the azimuth of $\vec{K}_S$ in relation to the direction of $\vec{k}_i$, then

$$K_1^2 = (2k_i)^2 + K_S^2 + 4\epsilon_2 k_i K_S \cos\theta_S$$

Hence at first order in K_S/k_i, i.e., at second order in F_S/f_B,

$$F_1 = f_B(1 + \epsilon_2 F_S^2 \cos\theta_S / 2f_B^2) = f_B + \epsilon_2 \phi$$

in which

$$\phi = (F_S^2/2f_B)\cos\theta_S$$

The spectral lines corresponding to the swell are at the respective frequencies [*Lipa and Barrick*, 1980],

$$f^{++} = f_B + F_S + \phi \qquad f^{+-} = f_B - F_S - \phi$$

$$f^{-+} = -f_B + F_S - \phi \qquad f^{--} = -f_B - F_S + \phi$$

where f^{++} and f^{+-}, and f^{-+} and f^{--} are symmetrical in relation to the corresponding Bragg frequency, i.e., f_B and $-f_B$, respectively, with distances equal to $F_S + \phi$ (positive lines) and $F_S - \phi$ (negative lines), and F_S and θ_S can be measured (except for the sign of θ_S because the geometric considerations influencing the positions of the lines are symmetrical in relation to the direction of the radar beam) by measuring the position of the four swell lines.

Figure 6 shows a characteristic example of experimental results in the Mediterranean. The frequency of swell is not much lower than that of wind waves, and the two can be separated by their time evolution. In this case, the peaks attributed to the swell have remained in the same position for several hours, while the second-order remainder has evolved via a decrease in the energy of the wind sea. The values of F_S and θ_S correspond to a swell having a period of 8 s and coming from the southwest or southeast, and they agree with the measurements made by the buoy and with direct observations.

Figure 7 shows two examples of experimental results in the Atlantic. The four swell lines can

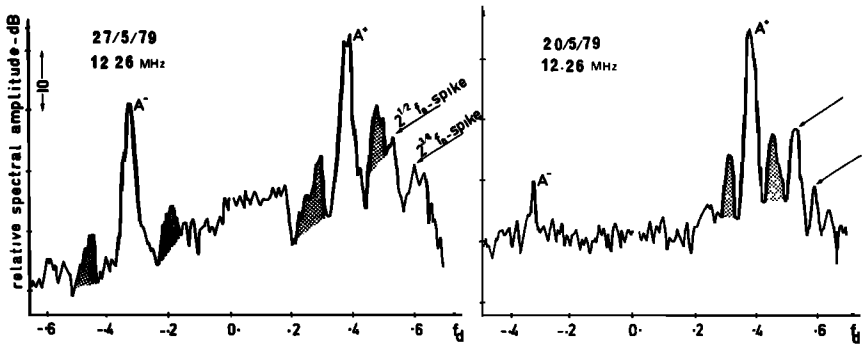

Fig. 7. Two Doppler spectra at 12.26 MHz for an Atlantic zone with four (left) and two (right) sharp swell spikes. Swell frequencies are 0.11 and 0.08 Hz, respectively. In both cases the swell propagates toward the radar station.

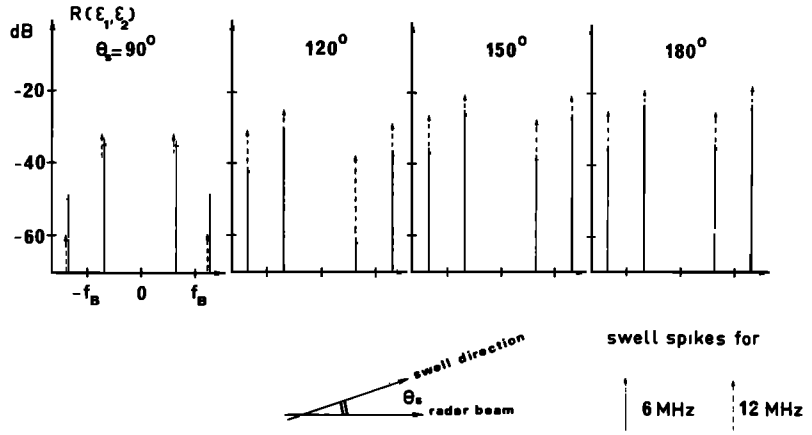

Fig. 8. Simulation for 6 and 12 MHz of the normalized amplitudes of swell spikes $R(\varepsilon_1, \varepsilon_2)$ (see text). Various angles of propagation θ_H are considered. The significant height H 1/3 is 1 m; the frequency of the swell if $F_S = 0.1$ Hz.

be seen on the left. They show a period of 8.8 s for the swell coming from the west. The negative swell lines on the right are under the noise level. This situation has been the most frequent one because the beam direction is the direction of the dominant winds (from the west). Nevertheless, the two positive lines lead to an estimate of F_H with an accuracy of approximately ϕ. The period is 12.5 $\pm$ 0.8 s. In both cases these values agree with the direct measurements.

Furthermore, the energy of these lines may be calculated as

$$\int E_S^{(2)}(f_d)\, df_d = 2\alpha_2 Th^2 S_W\{\varepsilon_1(-2\vec{k}_i - \varepsilon_2 \vec{K}_S)\}$$

whereas the energy of each of the Bragg lines is

$$\int E^{(1)}(f_d)\, df_d = \alpha_1 S_W(-2\varepsilon_1 \vec{k}_i)$$

The ratio of the energy of one swell spike to the energy of the nearest Bragg line is thus

$$R(\varepsilon_1, \varepsilon_2) = \frac{2\alpha_2}{\alpha_1} Th^2 \frac{S_W[\varepsilon_1(-2\vec{k}_i - \varepsilon_2 \vec{K}_S)]}{S_W[\varepsilon_1(-2\vec{k}_i)]}$$

If the Bragg frequency is sufficiently greater than the swell frequency, the vectors $-2\vec{k}_i$ and $-2\vec{k}_i - \varepsilon_2 \vec{K}_S$ have almost the same direction. The ratio of the spectral amplitudes of the corresponding waves can be evaluated by a simple model, for

TABLE 1. Comparison between swell parameters obtained via Doppler spectra (estimates) and by a pitch-and-roll buoy ('true values').

			Estimates			True values		
Date	Time (local)	Frequency (MHz)	F_H (Hz)	H_H (m)	θ_H	F_H (Hz)	H_H (m)	θ_H
			Atlantic Ocean					
May 20, 1979	1	12.3	0.08	1.5	180°	0.098	1.3	175°
May 21, 1979	23	12.3	0.11	1.9	180°	0.12	1.3	170°
May 27, 1979	5	12.3	0.13	2.3	180°	0.13	1.3	180°
May 27, 1979	6	5.9	0.11	2.7	180°	0.13	1.3	175°
June 4, 1979	7	12.3	0.10	1.4	180°	0.109	0.8	175°
June 4, 1979	14	5.9	0.095	1.2	180°	0.105	0.8	175°
June 6, 1979	20	5.9	0.12	0.8	180°	0.130	0.5	175°
June 7, 1979	12	12.3	0.11	1.8	180°	0.125	0.9	160°
			Mediterranean Sea					
December 7, 1978	0	12.8	0.125	1.1	140°	0.131	1.2	(Waverider buoy)

$H_H = 4 \times h$.

instance, Phillip's model, in which S is proportional to K^{-4}. The coefficient $R(\varepsilon_1, \varepsilon_2)/h^2$ is thus a given function of F_S, θ_S, f_B. If these parameters are known, the measurement of R enables h to be estimated, in principle. Figure 8 shows the values of R taken as a function of θ_S for a given radar frequency and swell frequency. Table 1 gathers the estimates made for swell parameters in May–June 1979 in the Atlantic compared to the direct measurements made by a pitch-and-roll buoy. It shows that h is always overestimated, with an average deviation of about 0.5 m, and that the agreement is quite satisfactory for the other parameters θ and F.

Actually, it should be noted that the swell frequency is the parameter which can be estimated with the greatest accuracy. Even if θ_S is unknown, this accuracy is approximately ϕ, i.e., less than $F_S^2/2f_B$, which is approximately 15% for currently observed values and a radar frequency of 12 MHz.

The measurement of θ_S is not done with the same accuracy, since ϕ is affected by an error which is at least equal to the spectral resolution (here 6×10^{-3} Hz), whereas its value is $1.4 \times 10^{-2} \cos \theta_S$ for a 10-s swell and a radar frequency of 12 MHz. So, only a few sectors of the swell propagation between 0° and 180° can be given by separating the cases for which ϕ is high (θ_S around 0° or 180°), small (θ_S around 90°), or intermediate (θ_S around 40° or 140°). The ratios R_{++}/R_{+-} or R_{-+}/R_{--} vary too little with θ_S, except when θ_S is near 90°, to improve this estimate for the case when only two swell spikes near one Bragg line can be observed (spectrum on the right of Figure 7, for example).

The estimate of h is most accurate around $\theta_S = 0°$ or 180° where the $R(\varepsilon_1, \varepsilon_2)$ ratios vary the least with θ_S. The experimental situation, in which the radar beam direction was almost the same as the direction of the most frequent swell ($\theta_S \approx 180°$), corresponded to this case.

6. CONCLUSION

The relation between the characteristic frequencies of the directional spectrum of the sea state (cutoff and peak frequency of the wind-driven sea, frequency of the swell) and the properties of the spectrum of the echo from the sea obtained by a HF Doppler radar were investigated from both the theoretical and experimental standpoints.

The simple equation ($f_0 = \pm f_B \pm F_0$) suggested by previous investigators is theoretically an approximation whose accuracy has been fully calculated for the cutoff frequency and the swell frequency.

Experimental results have proved that it was effectively possible to measure these frequencies and the dominant wave frequency with sufficient accuracy by analyzing the radar spectra. Nevertheless, some data for which the second-order spectrum did not fit the symmetry conditions required by the models used have had to be discarded. They probably correspond to directional patterns of the energy of the wind waves which do not spread energy in all directions at all the frequencies (models which give a significant amplitude only to the waves being propagated within a restricted-aperture cone around the wind direction, as described by *Lipa* [1978]). Under such conditions, the area in the plane (F_1, F_2) which contributes to the second-order echo is limited, and likewise the frequency extension of the echo is restricted.

Acknowledgments. This research received the support of Centre National de la Recherche Scientifique (ERA 668), Centre National pour l'Exploitation des Océans, Institut Français du Pétrole, Société Nationale Elf-Aquitaine (Production) and Compagnie Française des Pétroles (contract 1922-SNEA-P). Data from the directional pitch-and-roll buoy were provided by Centre Océanologique de Bretagne (CNEXO) in Brest, France.

REFERENCES

Barrick, D. E. (1972), Remote sensing of sea state by radar, in *Remote Sensing of the Troposphere*, U.S. Government Printing Office, Washington, D. C.

Barrick, D. E. (1977*a*), Extraction of wave parameters from measured HF sea-echo Doppler spectra, *Radio Sci.*, *12*(3), 415–424.

Barrick, D. E. (1977*b*), The ocean waveheight non directional spectrum from inversion of the HF sea-echo Doppler spectrum, *Remote Sens. Environ.*, *6*, 201–227.

Barrick, D. E., M. W. Evans, and B. L. Weber (1977), Ocean surface currents mapped by radar, *Science*, *198*, 138.

Broche, P. (1979), Sea state directional spectra observed by H. F. Doppler radar, *AGARD Conf. Proc.*, *263*, 31-1–31-12.

Crombie, D. D. (1955), Doppler spectrum of sea echo at 13.56 Mc/s, *Nature*, *175*, 681–682.

De Maistre, J. C., P. Broche, and M. Crochet (1978), Off-shore wind measurements by H. F. Doppler ground-wave radar, *Boundary Layer Meteorol.*, *13*, 55–60.

Hasselmann, K. (1971), Determination of ocean-wave spectra from Doppler radio return from the sea surface, *Nature*, *229*, 16–17.

Lipa, B. (1978), Inversion of second-order radar echoes from the sea, *J. Geophys. Res.*, *83*, 959–962.

Lipa, B. J., and D. E. Barrick (1980), Methods for the extraction of long-period ocean wave parameters from narrow-beam HF radar sea echo, *Radio Sci.*, *15*(4), 843–853.

Long, A. E., and D. B. Trizna (1973), Mapping of North Atlantic winds by H. F. radar sea backscatter interpretation, *IEEE Trans. Antennas Propag., AP-21*(5), 680–685.

Stewart, R. H., and J. R. Barnum (1975), Radio measurements of oceanic winds at long ranges: An evaluation, *Radio Sci., 10*(10), 853–857.

Stewart, R. H., and J. W. Joy (1974), H. F. radio measurements of surface currents, *Deep Sea Res., 21*, 1039–1049.

Tyler, G. L., W. E. Faulkerson, A. M. Peterson, and C. C. Teague (1972), Second-order scattering from the sea: Ten-meter radar observations of the Doppler continuum, *Science, 177*(4069), 349–351.